Transmission Line Matrix Modeling of Dispersive Wide-Band Absorbing Boundaries with Time-Domain Diakoptics for *S*-Parameter Extraction

ESWARAPPA, STUDENT MEMBER, IEEE, GEORGE I. COSTACHE, SENIOR MEMBER, IEEE, AND WOLFGANG J. R. HOEFER, SENIOR MEMBER, IEEE

Abstract—**A numerical modeling procedure based on Johns's time-domain diakoptics approach has been developed for efficient transmission line matrix (TLM) analysis of two-dimensional microwave circuits by introducing space interpolation techniques. Frequency dispersive boundaries are represented in the time domain by their characteristic impulse response or numerical Green's function (Johns matrix). Almost perfect wide-band absorbing boundary conditions have been obtained with this technique, permitting accurate characterization of waveguide discontinuities and components. The application of these techniques saves considerable computer run time and memory when compared with conventional TLM analysis.**

I. INTRODUCTION

THE TRANSMISSION line matrix (TLM) method is a numerical time-domain technique first described by Johns and Beurle [1] in which both space and time are discretized. The details of this method and an extensive list of references on this subject can be found in a review paper [2] and a book chapter on TLM [3] by Hoefer. New concepts and procedures which were developed to speed up TLM modeling were reported in [4]. The TLM method is very general in that it can cover arbitrary geometries and account for realistic features that are often neglected in theoretical analysis. The earlier applications of this method have concentrated mainly on finding the cutoff frequencies and propagation characteristics of transmission lines and resonant frequencies of cavities.

Only a few attempts have been made so far to compute scattering parameters with this method, since wide-band absorbing boundaries cannot be modeled in the time domain, particularly in structures supporting non-TEM modes of propagation. However, in the absence of a wide-band absorbing termination, the impulse excitation capability, which is one of the main assets of the TLM method, cannot be exploited. Furthermore, the wide-band absorbing boundaries must be of high quality since the Fourier transform of time-domain results is very sensitive to imperfect boundary treatment. Small errors in the time domain may produce fairly large errors in the frequency domain. Thus, even though the time-domain results may be reasonably accurate, the frequency-domain results obtained from their Fourier transform may not be acceptable as useful data. Therefore, simulation of good absorbing boundary conditions is very important for computation of *S* parameters.

Recently, absorbing boundary algorithms for the time domain–finite difference (TD–FD) method have been proposed in the literature [5]–[7]. In [7], even though the authors claimed less than 0.02% reflections from an absorbing boundary at a particular (tuning) frequency, they obtained less than 1% reflections only over a narrow bandwidth of 7.7% (center frequency $(\Delta l/\lambda) = 0.09$, bandwidth $(\Delta l/\lambda) = 0.007$) for TE_{10} mode propagation in a standard rectangular waveguide (Δl being the TLM mesh parameter and λ the free-space wavelength). In contrast, we have achieved less than 2% of reflections over the whole operating band of the waveguide with the method presented in this paper.

In the following, two different ways of modeling wide-band absorbing boundary conditions (matching terminations) in homogeneous waveguides will be described. Efficient implementations of wide-band absorbing boundaries using Johns's time-domain diakoptics approach with space interpolation techniques are presented in Section III. Then results for certain waveguide discontinuities and components computed with these techniques are presented in Section IV.

Manuscript received August 29, 1989; revised December 6, 1989. This work was supported by the National Science Engineering Research Council (NSERC) of Canada and the Telecommunications Research Institute of Ontario (TRIO).

The authors are with the Department of Electrical Engineering, University of Ottawa, Ottawa, Ont., Canada K1N 6N5.

IEEE Log Number 8934028.

0018-9480/90/0400-0379$01.00 ©1990 IEEE

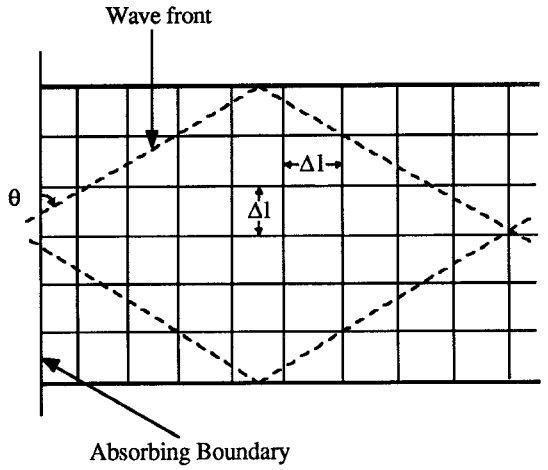

Fig. 1. Plane wave incident at an arbitrary angle θ.

II. Modeling of Wide-Band Absorbing Boundary Conditions

In the two-dimensional TLM simulation of a plane TEM wave, an absorbing boundary can be modeled by terminating the TLM mesh lines with the intrinsic impedance of the TLM mesh, $Z_0/\sqrt{2\epsilon_r}$, where Z_0 is the characteristic impedance of the mesh lines and ϵ_r is the relative permittivity of the simulated medium. This technique works well at all frequencies as long as the plane TEM wave is incident normally on the absorbing boundary and, of course, $\Delta l/\lambda$ is much smaller than unity. For a plane wave incident at an arbitrary angle θ (as in the case of waveguide modes, see Fig. 1), the mesh lines must be terminated with dispersive wave impedances $Z_0/\sqrt{2\epsilon_r(1-\sin^2\theta)}$, where ϵ_r is the relative permittivity of the medium filling the propagation space. Since this impedance is a function of the angle of incidence θ, the termination is totally absorbing only *at one frequency*.

To simulate absorbing boundaries over *a wide frequency range* in waveguides, we have employed two different approaches:

a) modeling of a waveguide termination with gradually increasing losses,
b) modeling of a very long uniform waveguide section.

A. Modeling of a Waveguide Termination with Gradually Increasing Losses

Practical waveguide terminations are made by arranging for the gradual absorption of the incident wave. A tapered resistive sheet or pyramid gradually increases the effective attenuation constant in the termination. Provided that the taper is made several wavelengths long, the reflection is very small. An alternative approach, more appropriate for modeling purposes, is to realize the termination by cascading a number of uniform lossy sections of waveguide as shown in Fig. 2(a). The loss tangent of the sections is progressively increased in such a way that reflection is minimized over a wide frequency range. We have obtained the required optimum loss profile using Touchstone™ CAD software. About nine sections of different lengths and loss tangents (the dielectric loss tangent is taken as the variable quantity) are needed to obtain a return loss of less than -40 dB over the operating band of a standard rectangular waveguide. The optimized lengths and dielectric loss tangents are given in Fig. 2(b). For a WR28 waveguide, the total length of the termination which consists of nine sections is 42.58 mm ($=3.785\lambda_g$ at the center frequency of the operating band). The return loss obtained with Touchstone is shown in Fig. 3. It is less than -40 dB throughout the operating band of the WR28 waveguide. The simulation of this lossy matched wave-

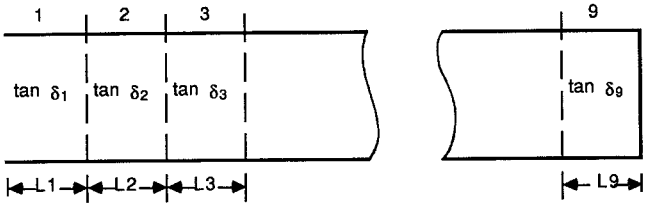

(a)

Section	Length (mm)	Dielectric Loss tangent (tan δ)
1	1.275	0.0095
2	1.739	0.0112
3	3.095	0.0499
4	3.031	0.1162
5	3.166	0.1990
6	7.980	0.2708
7	7.990	0.3686
8	7.536	0.8907
9	6.769	0.5960

(b)

Fig. 2. (a) Modeling of a wide-band absorbing waveguide termination by a cascade of nine increasingly lossy line sections. (b) Optimized lengths and dielectric loss tangents for a matched WR28 load (TE_{10} mode)

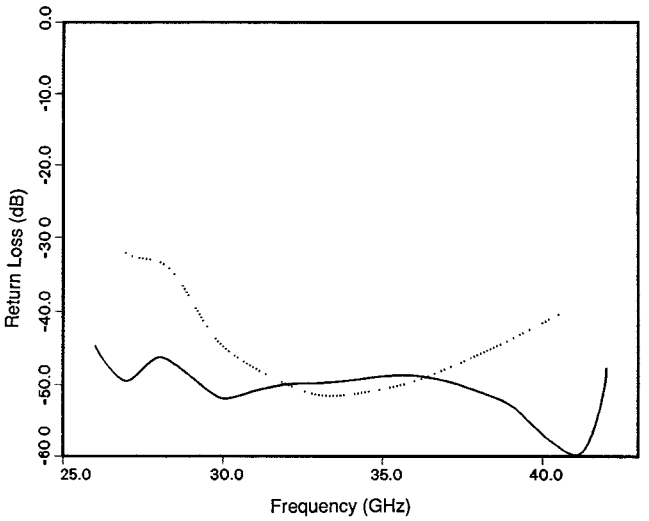

Fig. 3. Return loss of the lossy waveguide termination in Fig. 2: ——— simulation using Touchstone; · · · · · · simulation using TLM method.

guide termination with the TLM method is described below.

Simulation of the Lossy Waveguide Termination with the TLM Method: A TLM calculation usually starts by exciting the mesh at specific points by voltage or current impulses and follows the propagation of these impulses over the mesh as they are scattered by the nodes and bounce back at boundaries. Each iteration corresponds to a unit time Δt required for a pulse to travel from one node to the next. The output which is taken from a chosen point is a series of discrete impulses of varying magnitude separated by constant time intervals. This output function corresponds to a discrete sampling of the E field or H field (depending on the voltage or current) in the time domain. The frequency response (within any frequency range $\Delta l/\lambda$ much smaller than unity) can be obtained by performing the discrete Fourier transform on the output function. The TLM algorithm may be expressed as

$$_{k+1}[V]^r = S_k[V]^i + {}_k[V]^s \tag{1}$$

$$_{k+1}[V]^i = C_{k+1}[V]^r \tag{2}$$

where V^i and V^r are the incident and reflected impulses at the ports around the nodes at time step $k\Delta t$, S is a block diagonal scattering matrix for all nodes in the network, C is a connection matrix describing the topology of the network, and V^s is a source vector.

To account for dielectric losses, one can either consider the TLM mesh to consist of lossy mesh lines or load the nodes of a lossless mesh with so-called loss stubs [2], [3]. The latter approach has been adopted for our study, where each node is resistively loaded with a matched transmission line of appropriate characteristic admittance g_0, extracting energy from each node at every iteration. The values of g_0 are directly proportional to the local loss tangent and, for a lossy dielectric, can be derived as follows:

$$\epsilon = \epsilon_0\epsilon_r + \frac{\sigma}{j\omega} = \epsilon_0\epsilon_r(1 - j\tan\delta). \tag{3}$$

The conductivity, σ, of the medium and the equivalent attenuation constant, α, of the mesh lines can be expressed as follows:

$$\sigma \equiv \frac{g_0 cC}{\Delta l} \qquad \alpha = \frac{g_0}{4\Delta l\epsilon_r} \ \text{Np/m} \tag{4}$$

where g_0 is the normalized characteristic admittance of the loss stubs (normalizing admittance being the characteristic admittance of the main mesh lines) and Δl is the distance between nodes. The attenuation constant, α_n, of the network is

$$\alpha_n = \frac{g_0}{2\sqrt{2}\,\Delta l\sqrt{\epsilon_r}} \ \text{Np/m}. \tag{5}$$

The attenuation constant for dielectric losses can be written as [8]

$$\alpha_n = \frac{\omega^2\mu_0\epsilon_0\epsilon_r\lambda\tan\delta}{4\pi} \tag{6}$$

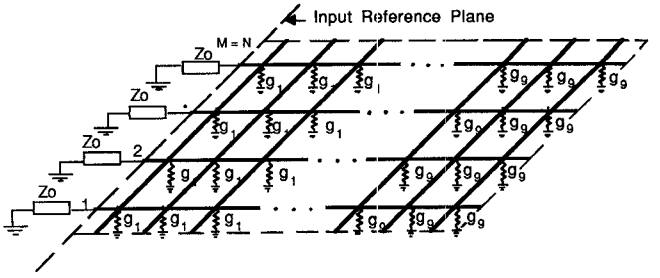

Fig. 4. Configuration for computing the discrete numerical Green's function or Johns matrix of a lossy waveguide matched termination.

where λ is the wavelength in the dielectric. From (5) and (6), g_0 follows:

$$g_0 = \frac{2\epsilon_r\sqrt{2}\,\pi f\Delta l\tan\delta}{c}. \tag{7}$$

If $\tan\delta$ and Δl are known, g_0 can be computed. The frequency can be taken as the midband frequency since g_0 does not change very much across the operating band of the waveguide. The only condition for (5) to (7) to be true is that

$$\alpha_n\Delta l \ll 1. \tag{8}$$

The TLM discretization of a matched termination (of Fig. 2) is shown in Fig. 4. Note that all boundaries are placed halfway between nodes to ensure time synchronism of impulses throughout the TLM mesh. The quantities g_1 and g_9 are the characteristic admittances of the loss stubs of sections 1 and 9, respectively. To satisfy the condition given by (8) and to keep the velocity error to a tolerable level, the width of the waveguide is discretized into $30\Delta l$ (i.e., $N = 30$ in Fig. 4), and about $180\Delta l$ are needed along the length to realize a WR28 waveguide matched termination (shown in Fig. 2(a)). The return loss obtained with a TLM simulation is given in Fig. 3. A minimum of 32 dB is obtained over the operating band of WR28 waveguide. That means the reflections off the absorbing boundary (input plane of the matched termination) are less than 2.5%. This proves the ability of the TLM method to properly account for the losses. The results can be further improved with finer discretization and more iterations.

B. Modeling of a Very Long Uniform Waveguide Section

In this approach, the wide-band termination is represented by a very long waveguide section, and computations are stopped before the reflections from the far end return to the reference plane. For example, for a computation covering 2000 iterations, we need to discretize a waveguide section which is $1000\Delta l$ long.

To compute the scattering parameters of a microwave two-port over a wide frequency band in a single TLM run, we need two absorbing boundaries, one at each port. If we wanted to include the absorbing TLM structures described above, the total additional length to discretize two absorb-

ing boundaries using approach A would be about $400\Delta l$, while for approach B it would be about $4000\Delta l$ (for a computation requiring 4000 iterations). That means we need enormous computer run time and memory to achieve the above absorbing boundaries with the conventional TLM algorithm. However, these problems can be solved effectively with less computer resources by using diakoptics and space interpolation techniques as described in the next section.

III. Implementation of Wide-Band Absorbing Boundary Conditions with Johns's Time-Domain Diakoptics Approach

A. Diakoptics Technique

Diakoptics (or segmentation) is a method of partitioning large structures into substructures which are solved independently and later reassembled. It is very attractive for the repeated analysis of large structures in which only a small subpart is changed from one problem to another. For example, during the optimization of planar and quasi-planar circuits, only the metallization part is changed, the homogeneous dielectric regions remaining unchanged. It is wasteful to analyze the entire structure every time a small change is made.

The method was originated by Kron [9] and has since been applied extensively in conjunction with frequency-domain methods [10]–[12]. For example, complicated two-dimensional planar components can be analyzed by segmenting them into regular shapes for which the analytical Green's functions are known. However, there are only a few regular shapes, and these applications are thus limited to certain standard regular geometries. The technique was extended to the time domain for TLM modeling by Johns and Akhtarzad in 1981 [13], [14]. They showed how the substructures may be solved in the time domain using the TLM method and how the reconnection is made. Since the characteristic impulse response (which can be interpreted as a numerical Green's function) of the substructures must be computed and stored, the extra dimension of time associated with the TLM method vastly increases the computer storage (when compared with steady-state problems). To reduce the computational effort, Johns and Akhtarzad proposed space approximations along the connecting interface: they connected only a fraction of the TLM branches in the interface. Using this space interpolation technique, they computed the cutoff frequencies of simple waveguides and ridge waveguides. Even though the computed values compared reasonably well with analytical values, the frequency response curve was no longer of $\frac{\sin(x)}{x}$ shape but got distorted because of loss/gain of power during the approximate connection process.

This shows that, even though the space-approximated diakoptics may work reasonably well for computing eigenvalues, it may introduce considerable errors in the computation of scattering parameters. For this reason, and in view of the comparatively large computer resources which are required for this method, there was not much further application of this technique.

Fortunately, the diakoptics technique can be made much more efficient and accurate in the case of single-moded transmission structures. Only a single removed branch in the interface is connected, and the field values at the remaining ports are interpolated according to the transverse mode field distribution. This reduces the computer storage and run time by a few orders of magnitude. These procedures are described next.

B. Application to Wide-Band Absorbing Boundaries

We have used diakoptics to represent wide-band matched terminations (shown in Fig. 4 and described in Section II) at the input reference plane by their time-domain characteristic impulse response or numerical Green's function. We then discretize only the circuit to be characterized and convolve its time-domain response with the numerical Green's functions in the input and output reference planes of the circuit.

The branches penetrating through the input reference plane (also called removed branches) are numbered 1 through $M = N$ (see Fig. 4). A single impulse injected at any of these branches will cause impulses separated by the iteration time interval to flow in streams out of the branches of this structure. These impulse functions result from the scattering at the nodes and boundaries of the structure, and can be interpreted as a Green's function in numerical form. All removed branches are terminated in their own characteristic impedance during this procedure so as to absorb the emerging output streams. If we denote $g(m, n, k)$ as the output impulse function emerging at the mth branch at $t = k\Delta t$ due to a unit excitation of the nth branch at $t = 0$, the complete Green's function for the input plane of the matched load can be written in matrix form as follows:

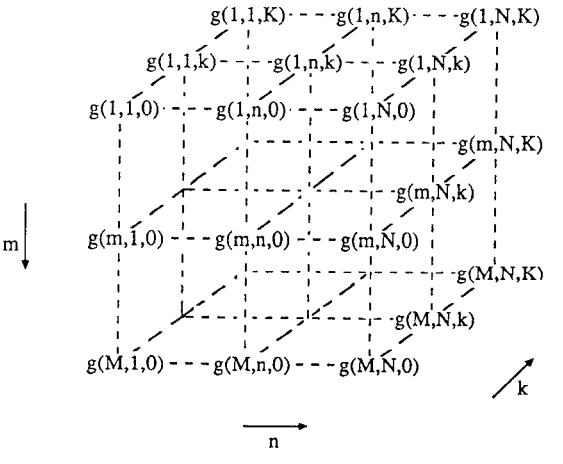

(9)

This is a three-dimensional array of dimension $(M * N * K)$, where K is the total number of iterations, and $M = N$ is the number of branches or transmission lines along the reference plane. We call this numerical Green's function a Johns matrix in honor of the late P. B. Johns, pioneer of TLM and time-domain diakoptics [4].

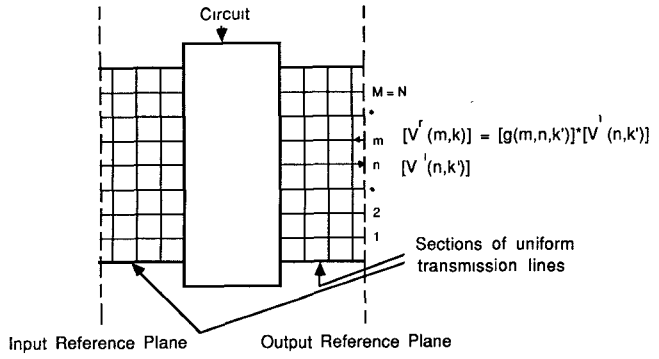

Fig. 5. Convolution of the Johns matrices of wide-band matched terminations with the impulse response of the circuit.

Note that the above matrix is computed only once and is stored. The next step is to discretize the circuit to be characterized and convolve its time-domain impulse response with these Green's functions (which simulate the wide-band absorbing boundary conditions in the time domain) along the branches of the input and output reference planes (see Fig. 5).

When impulses are injected into the circuit, they are scattered at nodes and boundaries and arrive after some time at the input and output reference planes. Any impulse which hits a reference plane will give rise to streams of impulses (characteristic of the matched termination) separated by the iteration time interval that will flow back into the structure through all branches. For example, a series of k impulses incident on the nth branch in the output reference plane will give rise to the following reflected impulse voltage on the mth branch:

$$\begin{aligned} V^r(m,k) = {} & V^i(n,k) * g(m,n,0) \\ & + V^i(n,k-1) * g(m,n,1) \\ & + \cdots + V^i(n,0) * g(m,n,k). \end{aligned} \quad (10)$$

This can be further written as follows:

$$V^r(m,k) = \sum_{k'=0}^{k} g(m,n,k') * V^i(n,k-k'). \quad (11)$$

The total reflected impulse voltage on the mth branch at time $k\Delta t$ due to the impulses incident on all N branches in previous iterations is the summation of the above term for N branches:

$$V^r(m,k) = \sum_{n=1}^{N} \sum_{k'=0}^{k} g(m,n,k') * V^i(n,k-k'). \quad (12)$$

The above equation forms the basis of the diakoptics algorithm.

The TLM algorithms with and without the diakoptics approach are shown in Fig. 6. Note the extra modules to be implemented for convolution purposes with the diakoptics approach. The computer run time and memory required with the conventional TLM algorithm (i.e., to discretize the circuit and two matched terminations together) is proportional to

$$(NX^c + 2 \times NX^m) \times N \times K \quad (13)$$

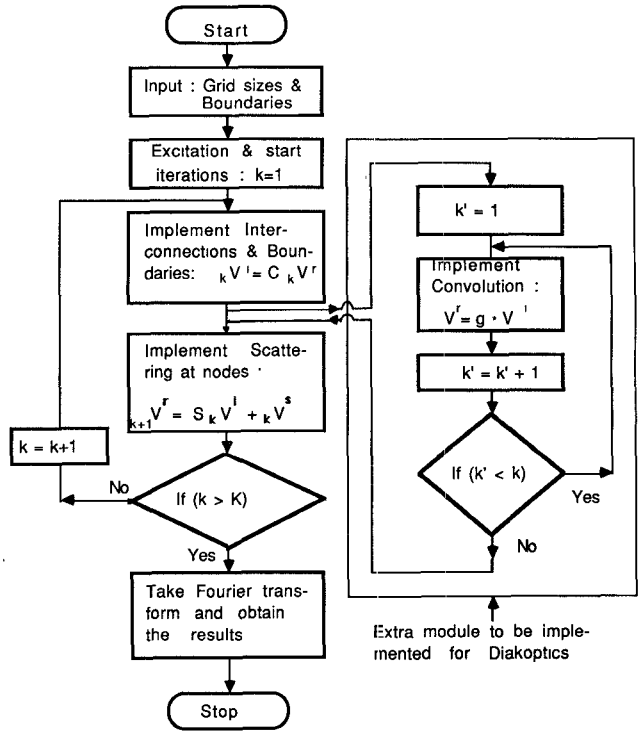

Fig. 6. TLM algorithms with and without diakoptics.

while that with the diakoptics technique is

$$(NX^c \times N \times K) + (K \times (K+1) \times N^2) \quad (14)$$

where NX^c is the number of grids along the length of the circuit and NX^m is the number of grids along the length of a matched load. In (14), the first term corresponds to the discretization of the circuit and the second part to the convolution with the Johns matrices of the matched loads.

The computer resources required for convolution can be reduced if we take the input and output reference planes far away from the circuit or discontinuity under test, so that we can assume only dominant mode propagation along the uniform guide (higher order mode effects on the transverse field distribution can be neglected). In such cases, if we excite the circuit at all the nodes along the input reference plane with impulses whose magnitudes are spatially distributed according to the dominant field distribution, the reflected impulses from these nodes at any iteration will have the same spatial distribution. Hence the impulse response of a matched load can be represented merely by storing the reflected impulse values at any one node for the required number of iterations. By knowing the transverse field distribution of the propagating mode (e.g., $\sin(\pi x/a)$ variation for TE_{10} mode propagation in waveguides), the reflected impulses at the other nodes can be calculated from these values. Hence the Johns matrix $G(M, N, K)$ becomes one-dimensional of size K, the total number of iterations. Thus the memory size required to store the Johns matrix is reduced by a factor of N^2 and the time taken to compute the Johns matrix is reduced by a factor of N, where N is the total number of branches along the reference plane.

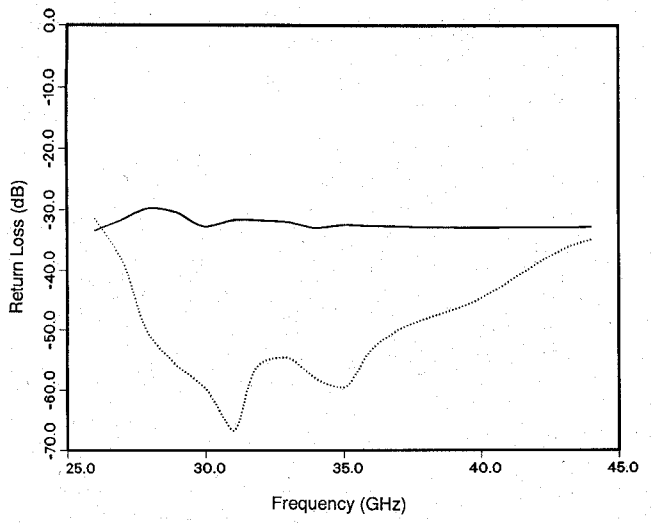

Fig. 7. Return loss of back-to-back waveguide absorbing boundaries computed with diakoptics: · · · · · · approach A; ——— approach B.

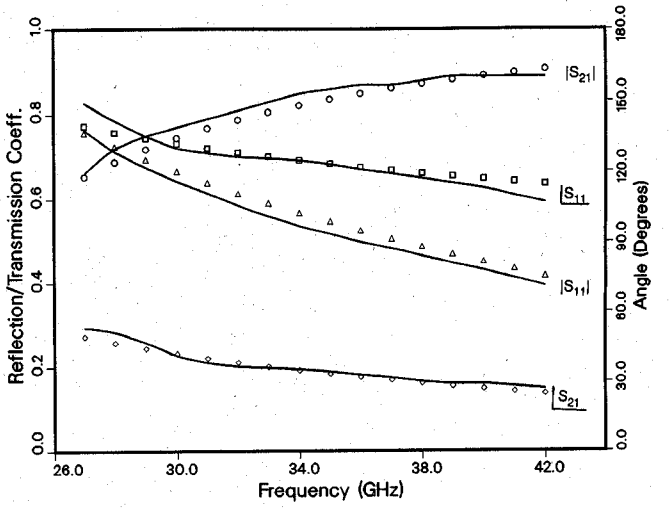

Fig. 8. S parameters of an inductive waveguide iris: ——— computed with diakoptics; ○□△◇ computed by Marcuvitz [15].

Note that in the convolution algorithm, we compute the reflected impulses (given by (12)) on all N branches along the reference planes in every iteration. The number of required computational steps is given by the second term of (14). However, under the above assumption, we can perform the convolution at only one node and calculate the reflected impulses at all other branches according to the spatial distribution of the dominant mode. Hence the time and memory taken to convolve are reduced by a factor of (N^2) and (14) becomes

$$(NX^c \times N \times K) + (K \times (K+1)). \tag{15}$$

Using the above technique, we have computed the return loss of the opposing absorbing boundaries (modeled as described in subsections II-A and II-B) separated by a length of WR28 waveguide (about $50\Delta l$ long). The return loss obtained as $20\log(VSWR-1)/(VSWR+1)$ is shown in Fig. 7. It is less than -35 dB throughout the operating band of the WR28 waveguide for approach A, while for approach B it is less than -30 dB, and the response is flat as expected. The propagation constant, β, can be obtained by solving

$$e^{-j\beta(\omega)(L_2-L_1)} = \frac{E_y(\omega, z=L_1)}{E_y(\omega, z=L_2)} \tag{16}$$

where L_1 and L_2 are the distances from the origin to any two points along the waveguide, and E_y are the Fourier transforms of $E_y(t)$ at $z=L_1$ and $z=L_2$. For the uniform WR28 waveguide, these β values agree exactly with the analytical values over the whole operating frequency band. Also, the phase difference of fields between any two consecutive nodes along the length of the waveguide is the same. This demonstrates the excellent quality of the wide-band absorbing boundaries.

IV. Applications

To further check the quality of the wide-band absorbing boundary conditions and to verify the validity of the proposed space interpolation techniques, we have computed the S parameters of an inductive waveguide iris discontinuity and an E-plane band-pass filter. The S parameters over the whole operating frequency band are computed with two TLM runs—with and without the discontinuity present. The incident field is obtained from analysis of a small section of the empty waveguide terminated on both sides with simulated wide-band matched terminations. The reflected field is obtained from the difference between the total field and the incident field.

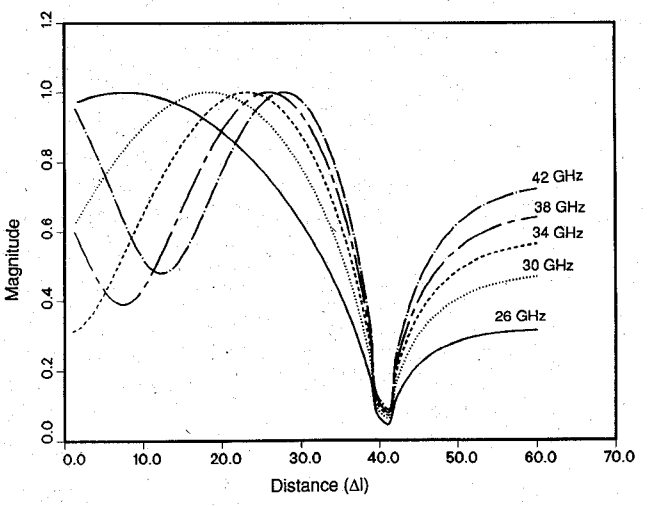

Fig. 9. Electric field variation along the length of a waveguide containing the inductive iris discontinuity at $40\Delta l$.

Fig. 8 shows computed magnitude and phase of the S parameters of a symmetrical inductive iris (of gap width equal to 3.556 mm) in a WR28 waveguide. Results compare well with those computed using empirical formulas given in [15]. The electric field variation along the center line of the waveguide around the inductive iris is shown in Fig. 9 for five different frequencies. Note a steep dip in the magnitude of the electric field at the discontinuity. The fields become almost constant for all frequencies on the right-hand side of the discontinuity, indicating the excellent quality of the matched loads. Fields vary sinusoidally

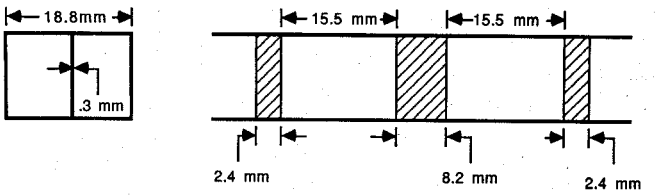

Fig. 10. The geometry of a two-section maximum flat *E*-plane filter.

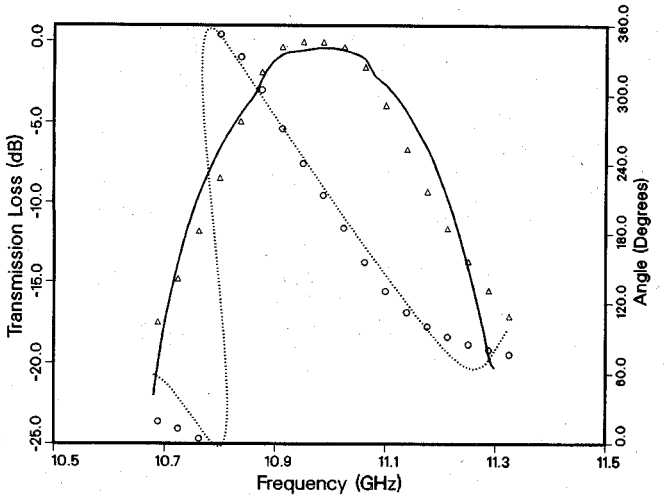

Fig. 11. Transmission characteristics of a *E*-plane filter: —— $|S_{21}|$ computed with diakoptics; · · · · · · S_{21} computed with diakoptics; △ $|S_{21}|$ computed with mode-matching technique (Uher); ○ S_{21} computed with mode-matching technique (Uher).

towards the left side of the discontinuity, as expected. Also, it can be seen that the higher order mode effect is almost negligible beyond a distance of about $20\Delta l$ on either side of the discontinuity.

Fig. 10 shows the geometry of a two-section maximum flat band-pass filter [16] with the following specifications:

center frequency:	10.95 GHz
bandwidth:	218 MHz
guide width:	18.8 mm
strip thickness:	0.3 mm

The computed transmission characteristics are given in Fig. 11. The results compare well with those computed with the mode-matching technique.

V. Conclusions

Excellent wide-band waveguide absorbing boundary conditions have been implemented using Johns's time-domain diakoptics approach. A space interpolation technique based on the dominant field distribution has been proposed for efficient *S*-parameter extraction. The good accuracy of this technique and the quality of wide-band absorbing boundary conditions are documented by the good agreement of the computed *S* parameters of waveguide components with data obtained with other methods.

Acknowledgment

The authors wish to thank J. Uher for computing the characteristics of the *E*-plane filter with his mode-matching program.

References

[1] P. B. Johns and R. L. Beurle, "Numerical solution of 2-dimensional scattering problems using a transmission-line matrix," *Proc. Inst. Elec. Eng.*, vol. 118, no. 9, pp. 1203–1208, Sept. 1971.

[2] W. J. R. Hoefer, "The transmission-line matrix method-theory and applications," *IEEE Trans. Microwave Theory Tech.*, vol. MTT-33, pp. 882–893, Oct. 1985.

[3] W. J. R. Hoefer, "The transmission line matrix (TLM) method," in *Numerical Techniques for Microwave and Millimeter Wave Passive Structures*, T. Itoh, Ed. New York: Wiley, 1989.

[4] P. So, Eswarappa, and W. J. R. Hoefer, "A two-dimensional TLM microwave field simulator using new concepts and procedures," *IEEE Trans. Microwave Theory Tech.*, vol. 37, pp. 1877–1884, Dec. 1989.

[5] J. Fang and K. K. Mei, "A super-absorbing boundary algorithm for solving electromagnetic problems by time domain finite difference method," in *Proc. AP-S Symp.*, June 1988, pp. 472–475.

[6] J. E. Roy and D. H. Choi, "The application of a simple absorbing boundary algorithm to cylindrical waveguide," in *Proc. AP-S Symp.* (San Jose), June 1989, pp. 58–61.

[7] J. E. Roy and D. H. Choi, "A simple absorbing boundary algorithm for the TDFD method with arbitrary incidence angle," in *Proc. AP-S Symp.* (San Jose), June 1989, pp. 54–57.

[8] R. E. Collin, *Field Theory of Guided Waves*. New York: McGraw-Hill, 1960.

[9] G. Kron, *Diakoptics*. London: MacDonald, 1963.

[10] T. Okoshi, Y. Uehara, and T. Takeuchi, "The segmentation method —An approach to the analysis of microwave planar circuits," *IEEE Trans. Microwave Theory Tech.*, vol. MTT-24, pp. 662–668, 1976.

[11] R. Chadha and K. C. Gupta, "Segmentation method using impedance matrices for analysis of planar microwave circuits," *IEEE Trans. Microwave Theory Tech.*, vol. MTT-29, pp. 71–74, 1981.

[12] R. Sorrentino, "Planar circuits, waveguide models, and segmentation method," *IEEE Trans. Microwave Theory Tech.*, vol. MTT-33, pp. 1057–1066, Oct. 1985.

[13] P. B. Johns and K. Akhtarzad, "The use of time domain diakoptics in time discrete models of fields," *Int. J. Num. Methods Eng.*, vol. 17 pp. 1–14, 1981.

[14] P. B. Johns, and K. Akhtarzad, "Time domain approximations in the solution of fields by time domain diakoptics," *Int. J. Numer. Methods Eng.*, vol. 18, pp. 1361–1373, 1982.

[15] N. Marcuvitz, *Wavegudie Handbook*. New York: Dover, 1965.

[16] Y. Konishi and K. Uenakada, "The design of a bandpass filter with inductive strip-planar circuit mounted in waveguide," *IEEE Trans. Microwave Theory Tech.*, vol. MTT-22, pp. 869–873, Oct. 1974.

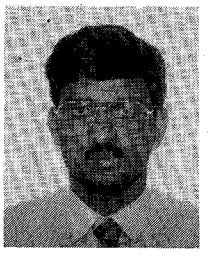

Eswarappa (S'89) received the B.E. degree in electronics and communication from Mysore University, India, in 1980 and the M. Tech degree in electrical engineering from the Indian Institute of Technology, Kanpur, in 1982.

From 1982 to 1986, he worked as an Assistant Executive Engineer in the Transmission Research and Development Laboratory, Indian Telephone Industries, Bangalore, India. He was mainly engaged in the design and development of microwave circuits and the characterization of microstrip discontinuities. Since 1986 he has been engaged in research on quasi-planar transmission media and numerical techniques, and he is working toward the Ph.D. degree in electrical engineering at the University of Ottawa, Ottawa, Ont., Canada.

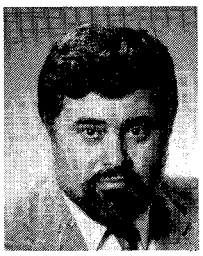

George I. Costache (M'78–SM'82) is a Professor in the Electrical Engineering Department at the University of Ottawa, Ottawa, Ont., Canada. His career has included positions with the University of Manitoba, the University of Manchester, and Electricitè de France. He has taught electromagnetics and numerical techniques applied to electromagnetics for more than 18 years and has made original contributions to the solution of skin-effect problems and electromagnetic transient phenomena. His main interest is in numerical techniques, such as finite-element analysis and moment methods, and their application to interference problems in steady-state and time-domain applications.

The author or coauthor of over 50 technical papers and reports, Dr. Costache is a member of the editorial review board of *COMPEL*, the international journal for computation and mathematics in electrical and electronics engineering. He is a registered Professional Engineer in the province of Ontario, Canada

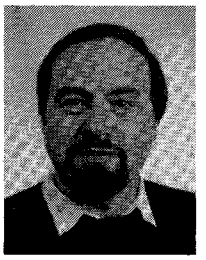

Wolfgang J. R. Hoefer (M'71–SM'78) received the diploma in electrical engineering from the Technische Hochschule Aachen, Aachen, Germany, in 1964 and the D. Ing. degree from the University of Grenoble, Grenoble, France, in 1968.

After one year of teaching and research at the Institute Universitaire de Technologie, Grenoble, France, he joined the Department of Electrical Engineering, University of Ottawa, Ottawa, Ont., Canada, where he is currently a Professor. His sabbatical activities have included six months with the Space Division of the AEG-Telefunken in Backnang, Germany, six months with the Electromagnetics Laboratory of the Institute National Polytechnique de Grenoble, France, and one year with the Space Electronics Directorate of the Communications Research Centre in Ottawa, Canada. His research interests include microwave measurement techniques, millimeter-wave circuit design, and numerical techniques for solving electromagnetic problems.

Dr. Hoefer is a registered Professional Engineer in the province of Ontario, Canada.